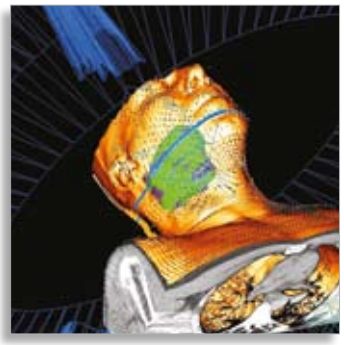

SmartArc

Background and algorithmic implementation of an efficient approach to volumetric arc therapy planning

Karl Bzdusek, David Robinson, and Michael Kaus, PhD of Philips Healthcare, Fitchburg, Wisconsin, USA

Henrik Friberger, Kjell Eriksson, and Björn Hårdemark of RaySearch Laboratories, Stockholm, Sweden

Corresponding author:
Karl Bzdusek
Philips Healthcare
5520 Nobel Drive
Fitchburg, WI 53711
Phone: (608) 288-6903
Fax: (608) 298-2101
E-mail: karl.bzdusek@philips.com

This article describes the foundation of the Philips SmartArc product, developed by Philips Healthcare and RaySearch Laboratories scientists. The first part of the article is based on the peer-reviewed scientific publications Bzdusek et al. (references 19 and 20). The algorithmic details, dosimetric plan results and delivery time estimates of the final product are very similar to those in this publication. The second part of the article provides additional detail on the optimization of the plan parameter variables, in the context of various dynamic arc delivery modes (constant or variable dose rate, constant or variable gantry speed, single or multiple arcs) and Elekta and Varian linear accelerators.

I. Introduction

Dynamic volumetric intensity modulated arc therapy (VMAT) evolved from intensity modulated arc therapy (IMAT) pioneered by Yu et al.[1] IMAT employed multiple coplanar arcs with constant dose rate, constant gantry speed, and multileaf collimator (MLC) segments derived from an IMRT optimization to create treatment plans with improved dosimetric quality for some treatment sites versus step-and-shoot IMRT. Linear accelerators now have the capacity to deliver VMAT, where MLC segments, dose rate and gantry speed, are varied simultaneously while the gantry is rotating. VMAT delivery has the potential to improve dosimetric fidelity and speed over step-and-shoot IMRT.[2-4] The technique promises dosimetric benefits for a wide range of disease sites, including prostate, head and neck, as well as other sites such as rectal, whole abdominopelvic, or endometrial.[1-8] Time saved at the treatment unit may be utilized towards image-guidance, online planning, and adaptive planning.

The additional degrees of freedom in VMAT require evolution of inverse planning optimization approaches as well. A concern with existing inverse planning approaches is the added complexity of the optimization parameter space. This can lead to long computation times and poor optimization results. The purpose of this work is to develop and characterize an efficient algorithm for generating dynamic arc plans that meet the clinical dosimetric requirements and improve delivery time. In this article, first the algorithmic components of plan optimization and arc sequencing are introduced. Ten plans for head and neck, prostate, brain, lung, and tonsil treatment sites are generated. The dynamic arc plans are compared to step-and-shoot IMRT direct machine parameter optimization (DMPO) plans based on dose distributions, dose volume histograms, and plan monitor units. Additionally, estimated arc delivery times and the overall plan generation times are recorded. The plans described in this article were not delivered, and even though they meet the published constraints of a specific machine, they may be undeliverable.[2]

PHILIPS

II. Methods and materials

II.A. Dynamic arc optimization overview

Dynamic arc optimization is achieved in several steps (Figure 1). After basic arc parameters, such as arc length and couch angle have been determined by the user, coarse segments around the arc are generated (section II.B). An intensity modulation optimization is performed on the fluence maps for these segments. The fluence maps are converted to MLC segments, two per angle (section II.C). The MLC segments are filtered, evenly redistributed around the arc, and interpolated segments are added to reach a final fine arc spacing. The resulting segments are optimized using machine parameter optimization to satisfy dose volume objectives and leaf motion, dose rate, and gantry speed constraints. Finally, convolution dose calculation (McNutt[9]) and segment weight optimization is performed to recover potential errors from the pencil beam dose calculation used during optimization. The result is a single dynamic arc "beam" that is deliverable within the linac's machine constraints.

II.B. Arc initialization and intensity modulation

The overall computation time is determined mainly by the discretization of the arc, that is the number of control points, and how close the initial solution is to the optimal plan. To limit computation time, we initially optimize intensity maps with a coarse angular resolution, then convert to MLC segments, and redistribute the segments around the arc at a finer resolution. The number of initial angles is guided by a trade-off of two characteristics: 1) Minimizing the number of initial angles has the potential to introduce large amounts of leaf travel per gantry angle rotation distance because segments generated from the initial intensity maps would be packed relatively close together, and 2) deriving MLC segments from a relatively small number of initial angles will limit intensity modulation, and may cause large initial errors when redistributing the segments because the converted segments would be positioned relatively far away from the intensity map from which it was generated.

To experimentally determine an optimal initial spacing, we varied initial arc spacing between 8° and 32° in four cases. The sensitivity of plan quality in terms of IMRT objective values in all four cases was small, but 8° spacing generally resulted in higher objective values. This is due to the fact that the smaller arc spacing resulted in more segments packed more tightly, and MLC leaves had to be adjusted to meet the leaf travel constraint. The optimal initial spacing of the arc fluence intensity segments was estimated to be about 24° and this measurement was used in all cases of this study.

With the initial spacing of the arc segments at 24°, the fluence maps are initialized to the target apertures and optimized using standard gradient based fluence optimization. Convergence was typically achieved after five to eight iterations.

II.C. Conversion and arc sequencing

Optimized fluence maps are converted to MLC leaf and jaw segments using a conversion algorithm that produces segments with leaf motion that travels from one side of the target to the other, also known as sliding window. The fluence is stratified into a number of equidistant discrete levels. The positions of each leaf pair which recreate the fluence are determined independently. The leaf positions are created in a leaf sweep fashion. In order to facilitate the creation of evenly shaped segments involving as many leaf pairs as possible, it is desirable that all leaf pairs have approximately the same number

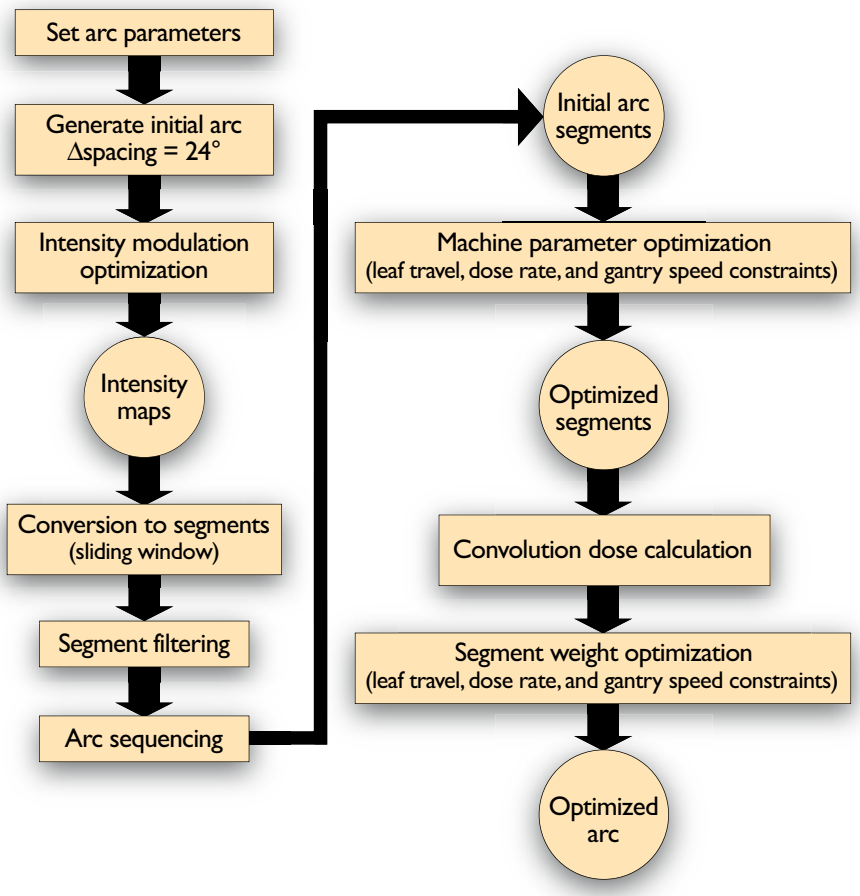

Figure 1: The dynamic arc optimization process

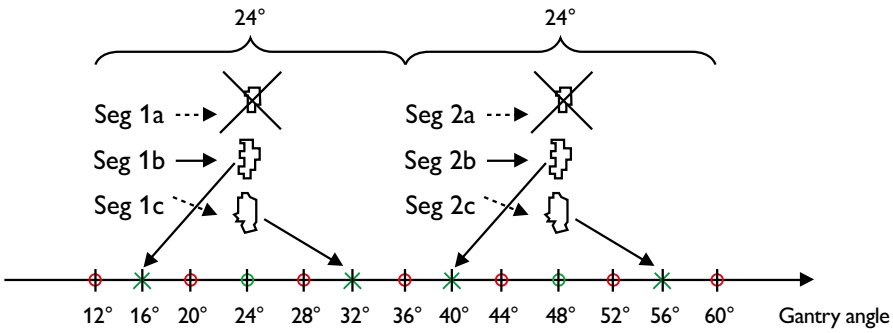

Figure 2: Segment filtering and redistribution. The optimized fluences at the initial directions of 24° and 48° are converted into three control points, respectively, where one segment is discarded and two are repositioned (crosses). Additional control points are created by linear interpolation of the leaves (light circles). The green control points are chosen for subsequent optimization. Another set of control points is introduced (dark circles) such that the final gantry spacing is 4°. The leaf positions and dose rates for these control points are not variables in the optimization; instead they are regenerated using interpolation every time dose or gradients are to be computed.

of openings, especially for the leaf pairs in the interior of the field. For this purpose, additional openings are created by the insertion of Steiner points.[10] Segments are built from openings in the different leaf pairs according to the mechanical constraints of the particular MLC, for example avoiding interdigitation.

Two to four segments per fluence map are generated depending on the degree of modulation. The created segments comply with all static machine constraints. Sliding-window segments were chosen because, by design, they dynamically transition from one MLC segment to the next. It was experimentally determined that two segments from each angle are sufficient to represent the intensity modulation and still be coarse enough to allow necessary leaf motion between segments. Using more than two segments resulted in large shape changes between segments and unacceptable leaf travel considering there are machine constraints for maximum leaf travel per degree and the maximum leaf speed. Using a single segment did not provide sufficient intensity modulation for more complex plans, and made it difficult or impossible to meet the prescribed dose volume objectives. Therefore, for each initial direction, the two segments with the highest number of open leaf pairs are selected and the remaining segments are discarded. The segments are assigned weights based on the outcome of the initial optimization. This focuses the initial segments on the largest target areas for each angle.

The two remaining control points from each initial direction are repositioned one third of the initial arc spacing to the left and to the right of the initial angle (Figure 2). Segments 1b and 1c are selected and repositioned and 1a is discarded. The control points are redistributed to the left or right such that overall MLC leaf travel is minimized. This is achieved by minimizing the mean leaf tip difference in the fields between adjacent segments.

Since an arc spacing resolution of less than 8° is required for dose calculation accuracy, interpolated MLC segments are inserted to achieve the final arc spacing resolution.[2] Additional control points with linearly interpolated leaf positions are added to maintain a distance between consecutive control points that is less than twice the defined final gantry spacing. This is typically 2 x 4° = 8°, totaling 46 control points if the arc length is 360° and an initial arc spacing of 24° is used. The 46 control points are included in the machine parameter optimization described in section II D.

Another second set of linearly interpolated control points is introduced in order to increase the dose computation accuracy. Thereby the user-defined final gantry spacing is reached, typically 4° resulting in 91 total control points at an arc length of 360°. To limit the optimization time and parameter space, and to assure smooth leaf transitions between consecutive control points, these control points are not part of the machine parameter optimization phase. Instead their leaf positions are regenerated using interpolation every time dose and gradients are to be computed.

II.D. Machine parameter optimization

After the MLC and jaw segments are created, machine parameters are optimized (Tables 1 and 2) using an iterative, non-randomized gradient based optimization algorithm (for example Gill[11]).[12] Optimization of the dose volume objectives is constrained by the commissioned machine specifications (MLC leaf speed, dose rate, gantry rate), where the explicit linear constraints are:

$$\left| l_{i+1,k} - l_{i,k} \right| \le \left| v_{max} t_i \right|$$

where

$$t_i = \frac{\Delta\theta_i}{\Delta\theta_{arc}} t_{arc}$$

$\Delta\theta_i \ge 0$ is the CP gantry angle interval and

$\Delta\theta_{arc} \ge 0$ is the arc gantry angle interval from start to stop, and

$$\left| l_{i+1,k} - l_{i,k} \right| \le \left| \delta_{max} \Delta\theta_i \right|$$

and the explicit variable bounds are

$$d_i \le d_{max} \qquad t_{arc} \ge \frac{\Delta\theta_{arc}}{\omega_{max}}$$

$$d_i \ge d_{min}$$

$$t_{arc} \le \frac{\Delta\theta_{arc}}{\omega_{min}}, \; if\_min > 0$$

$$t_{arc} \le t_{max}.$$

In addition to optimizing the leaf position parameters $l_{i,k}$ as done for step-and-shoot IMRT, total arc delivery time t_{arc}, and control point dose rate d_i are also optimized. The optimization can be performed on either (i) a fixed dose rate for the entire arc d_{arc}, or (ii) variable dose rates optimizing the individual control point (CP) dose rates d_i. In this study only variable dose rate was explored. The dose rates d_i can also be constrained to fall into discrete bins if the linear accelerator so requires.

Variable	Symbol
Leaf positions	$l_{i,k}$
Arc delivery time	t_{arc}
CP dose rate	d_i
Arc dose rate (constant for all CPs)	d_{arc}

Table 1: Dynamic arc optimization variables (CP – control point) (i = control point index, k = leaf index).

Dynamic arc specific constraints	Symbol
Maximum dose rate	d_{max}
Minimum dose rate	d_{min}
Maximum gantry rotation speed	ω_{max}
Minimum gantry rotation speed	ω_{min}
Maximum leaf speed	v_{max}
Maximum leaf travel distance per gantry degree	δ_{max}
Max arc delivery time	t_{max}

Table 2: Dynamic arc machine specific user specified constraints

Initial work suggested that predicting gantry speeds is difficult due to limitations in gantry acceleration and the variability between different linacs. Large gantry accelerations may introduce delivery errors and increase delivery times if the linear accelerator control system has to slow down to smooth the gantry acceleration. In addition, no machine information is available that describes how gantry speeds are varied versus dose rate. Several tests were performed comparing fixed gantry rates with variable gantry rates. It was determined that allowing the gantry speed to vary did not provide substantial plan improvement and is therefore constrained to a fixed value d_{arc}.

II.E. Dynamic arc specific machine parameter optimization constraints

The machine parameters used for this study are listed in Table 3. They represent the machine specifications of a Varian linear accelerator with 120 leaf interdigitating MLC and a variable dose rate. The maximum gantry rate was 6° per second and the minimum gantry rate was 1° per second although delivery time constraints limit this typically to a higher value. The maximum MLC leaf speed was chosen to 2.5 cm/sec although some newer machines may have higher limits. The maximum dose rate was 600 MU/min with the lower limit varying depending on the plan. In all cases the dose rate was continuously variable. The machine model used for this study did not include variable jaws.

Machine parameter	Constraint
Maximum gantry rate	6 deg/s
Minimum gantry rate	1 deg/s
Maximum MLC leaf speed	2.5 cm/s
Maximum dose rate	600 MU/min
Minimum dose rate varies per case	50–200 MU/min
Maximum leaf travel per degree	0.5 cm/deg

Table 3: Dynamic arc specific linear accelerator specifications used as optimization constraints.

II.F. Jaw positioning

After machine parameter optimization, the jaw positions for each segment are determined. For linear accelerators with constant jaws, the jaws are pushed to the extents of the most open leaf position for all segments. For linear accelerators with dynamic jaws, the jaw positions are determined for each individual segment. First, the closest jaw position to the most open leaf tip is determined. If the maximum jaw speed is less than the maximum leaf speed, the jaw position closest to the leaf tip is calculated that does not impact delivery speed, and the larger of the two jaw positions is chosen.

II.G. Estimating delivery time

The delivery time for the arc is a variable in the optimization with the goal of restricting it to a user-defined maximum value and to be able to ensure that leaf travel constraints are not violated. Hence the delivery time is a product of the optimization.

The delivery time value is an estimate since even though the control points are feasible with respect to all machine constraints, it is still up to the machine to interpret the control point information and determine what dose rate and gantry speed to use for each control point. Therefore, the actual delivery time may differ from the estimated value. Some specific examples include gantry acceleration limitations and machines that deliver a constant gantry speed plan created with our algorithm using a variable gantry speed.

II.H. Estimating optimization and dose calculation time

Computation times represent execution of the individual computational steps required in the overall process, that is initial arc creation, intensity modulation, arc sequencing, machine parameter optimization, adaptive convolution dose calculation, and segment weight optimization. These times do not represent the overall planning time which would include, for example, repeat adjustment of dose volume objectives and re-optimization to achieve a clinically optimal plan. Therefore the plan is reset after determination of all plan contributing elements, and above computational steps are executed and timed.

II.I. Pencil beam dose calculation

Pencil beam dose calculation contributes a substantial amount of the overall optimization time. In order to keep planning times clinically acceptable, a pencil beam algorithm was employed

based on the singular value decomposition (SVD) approach proposed by Bortfeld et al.[13] Further speed improvement is achieved by multi-threading the algorithm. Heterogeneities in the direction of the beam are taken into account. This algorithm has substantial performance gains compared to conventional pencil beam approaches (for example, Pinnacle 8.0m, Philips Radiation Oncology Systems, Fitchburg, WI), and reduced memory requirements to enable optimization with the large number of beam directions required for dynamic arcs.

III. Results and discussion

III.A. Treatment plan selection and dosimetric objectives

Ten step-and-shoot IMRT patient cases were selected for this study including three prostate, three head and neck, one brain, two lung cases, and one tonsil (Table 4). Patient cases were obtained from several clinical institutions including MD Anderson, Virginal Commonwealth University, and the University of Wisconsin. Plan complexity varied from a simple single target prostate case to a three-level tonsil case in order to represent a large percentage of cases that may benefit from dynamic arc therapy. The clinical beam arrangements, prescriptions, isocenter, and other plan parameters were used for the IMRT plans. The IMRT objectives were modified when it was possible to improve the plan, and none of these plans were used to treat patients. The beams in the IMRT plan were replaced by a single dynamic arc for the dynamic arc plans. Both the dynamic arc and IMRT plans were optimized using a research version of a commercial treatment planning software (Pinnacle, Philips Radiation Oncology Systems, Fitchburg, WI). Step-and-shoot IMRT plans were optimized using direct machine parameter optimization (DMPO).[12] Dynamic IMRT or sliding-window plans were not considered in this study.

Step-and-shoot IMRT plan objectives received from clinical institutions were used as the starting point and modified to take advantage of the added capacity of dynamic arcs to produce conformal dose distributions. Both the step-and-shoot IMRT plans and the dynamic arc plans have objectives optimized for the respective delivery modality but in general they are similar. A significant attempt was made to ensure optimal plans were generated for both the IMRT and dynamic arc plans. The objectives were chosen according to the following guidelines derived in part from RTOG studies:[14-17]

Prostate

Primary goals: Maintain the rectal dose at V70 Gy < 20%, while maintaining uniform dose to the prostate PTV. Secondary goals: Minimize bladder and femoral head dose.

Head and neck

Primary goals: Maintain the dose to the parotid gland to a clinically acceptable level, spare the cord and brainstem as much as possible, cord maximum dose 4500 cGy, brainstem 5000 cGy, and achieve uniform target dose for all levels and glands. Secondary goals: Reduce dose to all other critical structures such as optic nerve and optic chiasm, with objectives according to the clinical step-and-shoot IMRT plan.

Lung

Primary goals: Uniform PTV dose, maximal sparing of the cord, the heart, and the esophagus. Secondary goals: Maximize lung sparing V20 Gy < 20%.

Brain

Primary goals: Uniform dose to the PTV. Spare the cord and brainstem. Secondary goals: Reduce dose to other critical structures such as the optic chiasm.

Tonsil

Primary goals: Uniform dose to all PTV levels. Spare parotid glands and spinal cord. Secondary goals: Reduce dose to all other critical structures such as larynx and mandible with objectives according to the clinical step-and-shoot IMRT plan.

III.B. Dynamic arc treatment plan results

The ten clinical treatment studies were optimized for both step-and-shoot IMRT and dynamic arc delivery. The plans were compared based on dose distributions, clinical objectives, dose volume histograms, and plan monitor units. Additionally, estimated arc delivery times and the overall plan computation times were determined.

The objectives for the two delivery types were similar but tailored to the particular modality. In some cases, additional maximum dose objectives on the targets were introduced for the dynamic arc to avoid hot spots, but rotating the collimator to 45° or 90° usually had a similar effect. In this study, tailoring dynamic arcs was more achievable due to the increased degrees of freedom from the relatively large number of arc angles. But to achieve this, several more objectives were necessary, increasing the optimization problem, resulting in a longer optimization time.

All dynamic arc plans consisted of a single 360° arc except for the brain study which used a 225° arc to avoid direct irradiation of the eyes and mouth. Collimator angles varied for each study and the couch angle was 0° for all plans. A summary of the plan parameters is listed in Table 4. Dosimetrically, the dynamic arcs were typically superior, or similar, to the corresponding step-and-shoot IMRT plan. Target coverage was similar in almost all cases, but better critical structure sparing was achieved for some structures. In addition, as with all rotational therapies, integral dose was generally more evenly distributed with fewer hot spots and substantial increases or decreases were not noticed. Monitor units were lower for dynamic arc plans for a majority of the cases, but there were several exceptions notably one prostate case.

For the three head and neck nasopharynx cases, the differences in target doses between the two delivery types were similar, but in the majority of the cases the dynamic arcs tended to have a slightly higher maximum dose and slightly lower minimum dose (Table 5). The primary CTV 72 in HN1 includes the GTV + 0.5 cm and the CTV 49.5 includes the primary CTV and lymph nodes. The primary GTV 70 in HN2 includes part of the right lymph nodes. The CTV includes the GTV with an asymmetric margin that ranges from about 0.5 cm near the skin surface to up to 1.5 cm near the trachea and the right lymph nodes. A small volume of the mandible is included in the CTV. The left lymph nodes are treated as a separate target. The GTV in HN3 is located to the left of the trachea, and the CTV 72 includes the GTV and a uniform margin of 0.5 cm with the exception of an extension to include the left lymph nodes. The CTV 49.5 includes CTV 72 and all of the lymph nodes. In all three cases, improved sparing for one or more critical structures was achieved. For example, the dose around the spinal cord and brainstem tended to have more conformity and margin for dynamic arcs. The high dose tended to push further from the structures, making the plan more robust to potential setup errors and anatomical patient changes (Figures 3 and 4). The maximum dose was often substantially lower for these structures, for example the cord dose for HN2 was reduced from 3610 cGy to 2375 cGy (Table 5). In some cases, substantially improved parotid and mandible sparing was achieved using dynamic arc optimization. For example, the parotid EUD in HN3 was reduced from 2325 cGy to 1738 cGy using an "a" value of 1.[18] The monitor units for all three HN plans were reduced by 5–15%. Finally, the second head and neck plan had a large CTV that could not be covered by a single MLC segment for several beams in the IMRT plan. These beams were split into two. A single arc was needed to achieve target coverage for the dynamic arc plan.

Treatment site	Target dose (cGy)	Fractions	Optimization	Collimator angle (deg)
Nasopharynx 1 HN	UD CTV 7200 (Tgt1)	40	IMRT	0
1, 7 beams	D97 CTV 4950 (Tgt2)		Dynamic arc	0
Nasopharynx 2 HN	UD GTV 7000 (Tgt1)	35	IMRT	0
2, 7 beams	D98 CTV 6500 (Tgt2)		Dynamic arc	0
	D98 Nodes 5400			
Nasopharynx 3 HN	UD CTV 7200 (Tgt1)	40	IMRT	180
3, 7 beams	D97 CTV 4950 (Tgt2)		Dynamic arc	10
Prostate 1, 7 beams	UD PTV 7600 (Tgt1)	38	IMRT	0
	D95 Nodes 5400 (Tgt2)		Dynamic arc	10
Prostate 2, 5 beams	UD Prost 8000 (Tgt1)	40	IMRT	0
	MD PTV 7000 (Tgt2		Dynamic arc	0
Prostate 3, 5 beams	UD PTV 8000 (Tgt1)	45	IMRT	0
	MD PTV 6300 (Tgt2)		Dynamic arc	10
Tonsil, 7 beams	UD CTV 6600	33	IMRT	0
	MD CTV 6000		Dynamic arc	90
	D96 CTV 5400			
Brain, 6 beams	UD PTV 2500	5	IMRT	0
			Dynamic arc	0
Lung 1, 11 beams	UD PTV 3600	6	IMRT	270
			Dynamic arc	180
Lung 2, six beams	UD PTV 6600	30	IMRT	180
			Dynamic arc	10

Table 4: Treatment plan summary (MD = minimum dose, UD = uniform dose, DX = dose X % of volume)

The three prostate studies showed similar target doses for step-and-shoot IMRT and dynamic arc optimizations (Figure 5 and Table 6). Targets and PTV margins varied depending on the IMRT plan and the originating institution. For the prostate plan 1 the primary target includes a PTV with a 1 cm margin around the prostate and seminal vesicles except at the boundary with the rectum where it is 0.5 cm and it excludes the pelvic bone. For prostate plan 2 the primary target includes the prostate with no margin and the PTV includes the prostate

	Tgt 1		Tgt 2		Nodes					
Case	D95% (%PD)	max (%PD)	D95% (%PD)	max (%PD)	D95% (cGy)	max (cGy)	Cord max (cGy)	Parotid EUD	BS max (cGy)	MU
HN 1 IMRT	97.6	104.2	99.5	104.2	-	-	2247	2109	5872	547
HN 1 Arc	97.1	104.2	97.1	107.7	-	-	2159	1833	5231	458
HN 2 IMRT	98.1	105.4	96.6	108.8	99.4	104.0	3610	1976	3337	572
HN 2 Arc	97.9	104.3	96.8	105.5	98.3	103.5	2375	1955	2469	546
HN 3 IMRT	97.4	103.2	103.3	104.6	-	-	2745	2325	5832	537
HN 3 Arc	97.1	104.8	100.1	106.1	-	-	2454	1738	5391	494

Table 5: Head and neck studies (%PD = Percentage of prescription dose, BS = Brainstem)

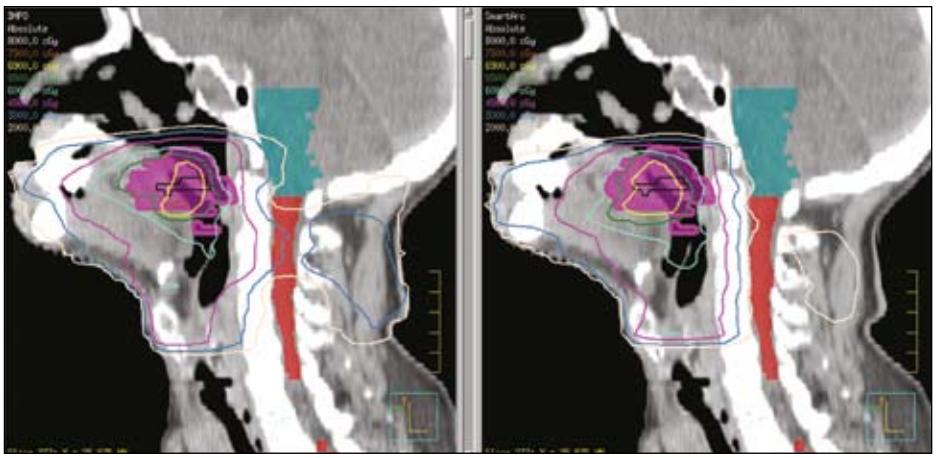

Figure 3: Nasopharynx plan 2. Left: step-and-shoot IMRT. Right: Dynamic arc. The dose conformality around the cord and brainstem was improved in the dynamic arc plan while preserving target dose uniformity. Some higher dose was noted below the target in all three arc plans.

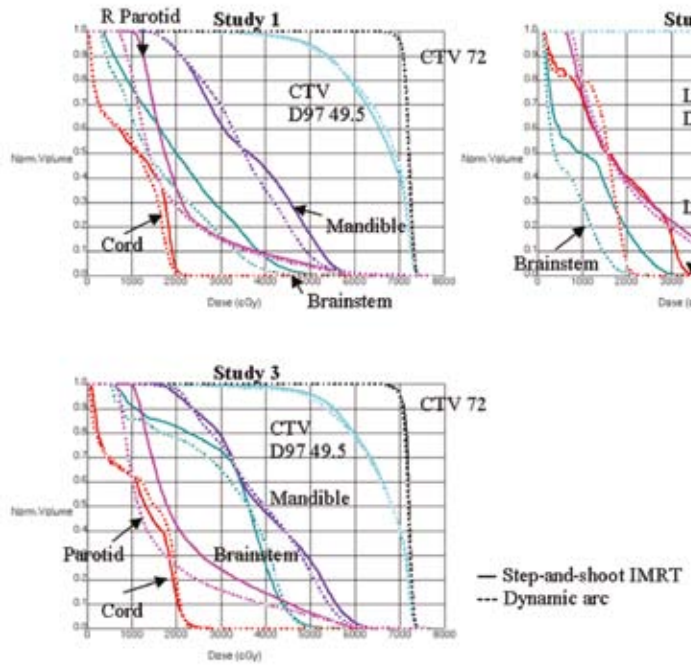

Figure 4: Dose volume histograms for the three nasopharynx studies. Target doses were clinically comparable while some of the critical structures such as the cord in study 2 had clinically relevant sparing improvements.

and seminal vesicles with a uniform 1 cm margin that includes the pelvic bone. For the prostate plan 3 the primary target includes the prostate with a 1 cm margin except at the boundary with the rectum where it is 0.5 cm and it includes the pelvic bone. There is a second PTV that includes PTV 1 and the seminal vesicles with a 0.5 cm margin. As with the head and neck studies, the arc target doses were slightly less uniform but not clinically relevant. Rectal and bladder sparing was also comparable, but two of the arc plans showed improvements in the high-volume low-dose region for the rectum. At the bladder V75 Gy the % volume was nearly identical and at the rectal dose V70 Gy the % volume was slightly higher (1-2%) for the arc plans. In all three cases there were improvements in femoral head sparing (Figure 5). Similar or better femoral head sparing for the IMRT plans could be achieved with different beam arrangements, but it always came at the expense of degradation to the target dose uniformity. Each prostate case has a different beam arrangement so differences between the step-and-shoot IMRT and the dynamic arc plans seem to be consistent. Two of the three prostate cases had a reduction in monitor units relative to the step-and-shoot IMRT plans, while the third case had significantly lower MUs for the step-and-shoot plans (~23%).

The two lung cancer studies once again showed that similar target doses could be achieved with step-and-shoot IMRT and dynamic arc optimizations (Figures 6, 7, Table 7). The GTV for lung study 1

Case	Tgt 1 D95% (%PD)	Tgt 1 max (%PD)	Tgt 2 D95% (%PD)	Tgt 2 max (%PD)	Bladder v75 Gy (%)	Rectum v70 Gy (%)	MU
Prostate 1 IMRT	96.4	106.3	99.6	104.1	6.3	8.3	649
Prostate 1 Arc	96.5	108.3	95.6	106.7	6.4	9.2	602
Prostate 2 IMRT	99.4	101.1	100.4	101.0	6.4	8.6	416
Prostate 2 Arc	99.6	102.9	100.6	102.4	6.7	9.3	395
Prostate 3 IMRT	100.8	103.4	108.3	105.2	10.4	12.8	348
Prostate 3 Arc	100.5	105.1	107.1	105.1	11	14.3	450

Table 6: Three prostate studies (%PD = Percentage of prescription dose)

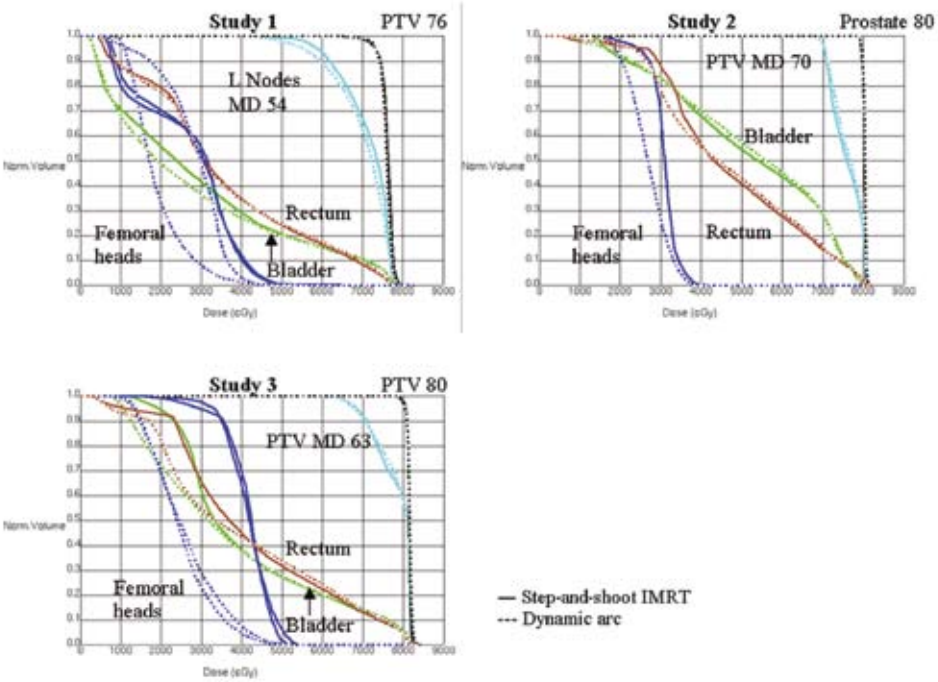

Figure 5: Dose volume histograms for three prostate studies. Target doses, rectal sparing, and bladder sparing were clinically identical for both delivery types. Femoral head sparing was clinically substantially improved for the arc plans.

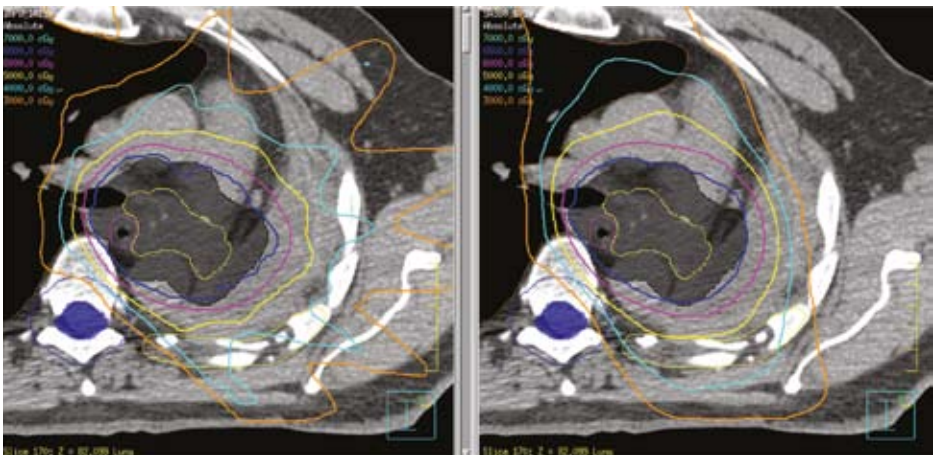

Figure 6: Dose distributions for lung study 2. Left: Step-and-shoot IMRT. Right: Dynamic arc. The distributions show improved conformal target coverage and smaller regions of integral dose for dynamic arcs. The high dose region was slightly closer to the spinal cord in the arc plan.

is a large mass in the right lung about 2.5 cm superior to the diaphragm. The PTV extends the target by a uniform 0.5 cm margin. The GTV for lung study 2 is located about 1 cm superior to the heart and the PTV extends the GTV with an anisotropic margin between 1 and 2 cm. The margin is reduced near the heart and the vertebrae. Slight improvements were made in some critical structure sparing with the esophagus showing the largest improvement. Dynamic arc planning reduced MUs for the first lung study by about 23%, but only 7% for the second study.

The step-and-shoot IMRT and dynamic arc optimizations were very similar for the brain study. The GTV is located in the posterior section of the brain and the PTV extends left and towards the anterior by about 1.5 to 2.5 cm. The unextended sections of the GTV have a uniform 0.5 cm margin. The dose to the PTV was slightly more uniform for the step-and-shoot IMRT. This is highlighted by the maximum PTV dose (Table 8) and the dose volume histograms (Figure 8). The cord and brainstem sparing was very similar. All other critical structures were almost fully avoided by both optimizations. Monitor units were reduced by about 13% using a dynamic arc.

The tonsil study showed many similarities to the nasopharynx studies. The GTV is the right tonsil and the CTV 66 extends the GTV by an asymmetric margin that avoids the mandible but is mostly 0.5 cm. The CTV 60 extends CTV 66 by including the right lymph nodes. CTV 54 is a small target that includes part of the left tonsil. Target doses were similar with improvement on some of the critical structure sparing (Figure 9, Table 9). Most notably, the maximum cord dose was reduced from 4613 cGy to 4349 cGy and the maximum brainstem dose from 5814 cGy to 5300 cGy. Monitor units for both plans were nearly identical.

III.C. Dynamic arc treatment plan delivery and optimization results

Combined optimization and dose calculation times varied from 5 to 20 minutes for all dynamic arc studies. Most optimizations were 13 minutes or less with the exception of the lung cases. In these cases an additional adaptive convolution dose was carried out after the arc conversion in order to improve on the heterogeneity achieved with pencil beam dose calculations during optimization. Other parameters that impacted computation time were the target size and the number of objectives. The dynamic arc optimization took approximately three to four times longer than step-and-shoot IMRT optimizations which typically range from 2-6 minutes. All estimated delivery times were between 70 and 120 seconds (Table 10) based on machine specifications of a Varian linear accelerator with variable dose rate.

Case	PTV D95% (%PD)	PTV max (%PD)	Lung v20 Gy (%)	Heart max (cGy)	Cord max (cGy)	MU
Lung 1 IMRT	93.9	107.8	2	1496	2102	1420
Lung 1 Arc	95.3	108.4	3	1404	2020	1098
Lung 2 IMRT	98.2	104.0	9	6255	2754	440
Lung 2 Arc	98.6	103.6	9	5666	2917	409

Table 7: Summary of two lung studies (%PD = Percentage of prescription dose)

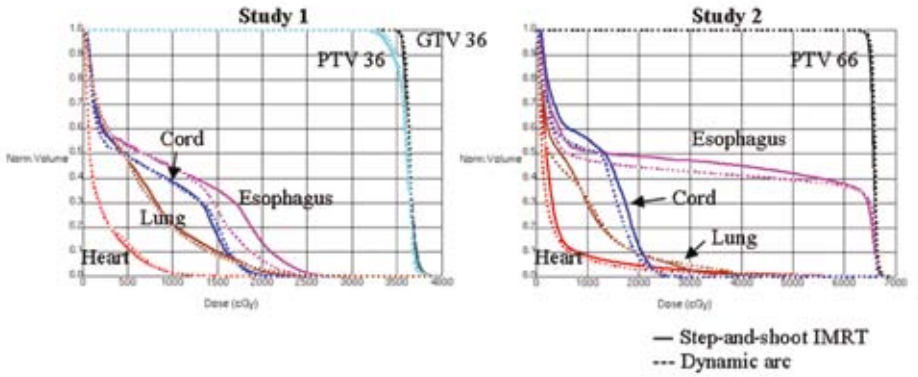

Figure 7: Dose volume histograms for two lung studies

Case	PTV D95% (%PD)	PTV max (%PD)	Cord max (cGy)	Brainstem max (cGy)	MU
Brain 1 IMRT	98.0	102.4	309	784	983
Brain 1 Arc	98.0	103.6	261	739	854

Table 8: Brain study summary (%PD = Percentage of prescription dose)

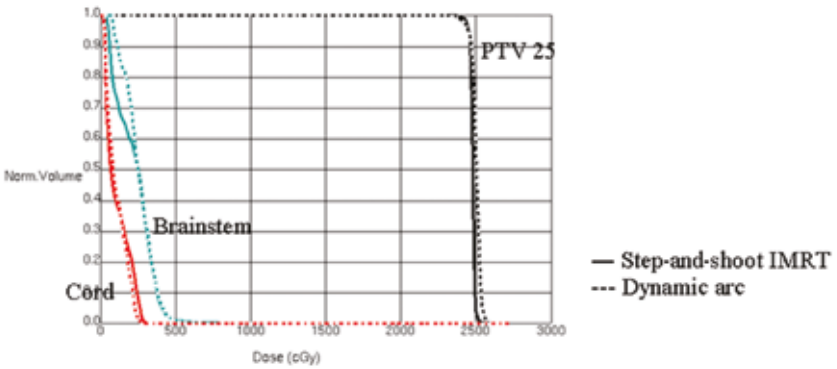

Figure 8: Dose volume histogram for the brain study showed lack of target dose conformality for the arc case but some improvement in critical structure sparing.

IV. Discussion

The results from 10 treatment studies showed that plan quality similar to, or better than, traditional step-and-shoot IMRT can be achieved with a single dynamic arc of 360° gantry rotation or less. In all studies the target dose was clinically comparable for both delivery types. An attempt to manually optimize the collimator angle for the brain case was made, exhibiting substantial sensitivity with the optimal angle of 0°. The sensitivity was mostly due to geometric alignment of the MLC with the target and critical structures. This data was not included in the study.

The dynamic arc, in many cases, was able to achieve better critical structure sparing in one or more organs at risk. This behavior varied with the particular plan but overall the most success was seen in the spinal cord, brainstem, and femoral heads.

Plan quality improvements may also be achieved by optimizing all of the interpolated segments generated during conversion. For this article, only a subset of the segments is optimized primarily to assure smooth leaf transitions between control points (section IIC). Recent work indicates that this not necessary and that all segments can be optimized while constraining leaf motion. This is a subject for future work.

Dynamic arc planning tended to enable improved tailoring of high-volume, low-dose regions because of its flexibility to spread out the dose at many beam angles. This reduces the need for structures defined specifically to remove dose hot spots, thus reducing overall planning effort.

For plans with up to three target levels, delivery times of less than two minutes were achievable. The effect of increasing the delivery time in favor of improved dosimetric plan quality was not studied but is a viable option in clinical practice. Only one lung plan was allowed a 160 second delivery time estimate.

Increasing the arc sampling rate from 4° to 2° may further improve plan quality, resulting in twice as many dose calculations and, in case all segments are optimized, doubling the number of optimization parameters. This approximately doubles the plan optimization and dose calculation times. We speculate that only certain cases, for example with complex target shape requiring substantial leaf motion, would benefit from such modifications.

Case	CTV66 D95% (%PD)	CTV66 max (%PD)	CTV60 D95% (%PD)	CTV60 max (%PD)	CTV54 D95% (%PD)	CTV54 max (%PD)	Cord max (cGy)	L Parotid EUD	Brainstem max (cGy)	MU
Tonsil 1 IMRT	99.1	104.6	100.0	104.6	98.9	108.2	4613	1273	5814	418
Tonsil 1 Arc	99.1	105.4	99.8	105.4	99.3	109.7	4349	1271	5300	414

Table 9: Tonsil study summary (%PD = Percentage of prescription dose)

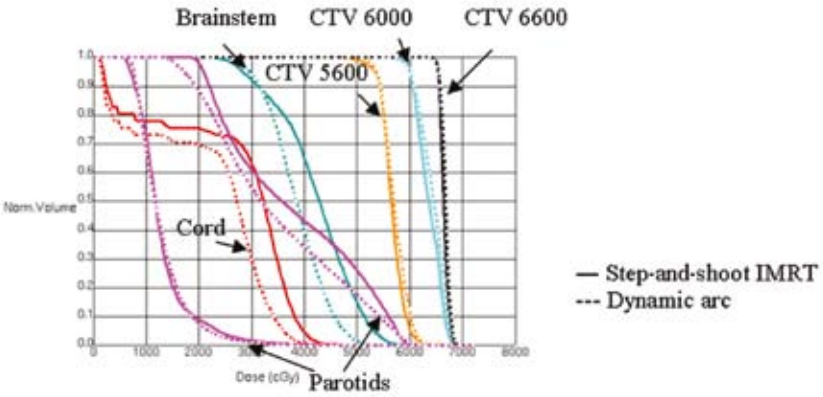

Figure 9: Dose volume histograms for the tonsil study. Target doses were clinically identical for both optimization methods. There was clinically relevant improved sparing for several critical structures such as the spinal cord and brainstem using a dynamic arc.

	Combined opt and dose calc time (min)	Estimated delivery time (sec)
Nasopharynx 1	12.3	113
Nasopharynx 2	13.2	120
Nasopharynx 3	11.6	120
Prostate 1	11.2	120
Prostate 2	11.6	70
Prostate 3	11.9	60
Tonsil	10.3	112
Brain	4.7	120
Lung 1	19.5	160
Lung 2	35.1	87

Table 10: Optimization and estimated delivery times for dynamic arc plans. Optimization times for corresponding IMRT plans range from 2-6 min.

The optimization flexibility for critical structure sparing was explored by reducing the objective weights and substantially lowering the maximum dose or maximum DVH objective dose levels. This allowed the optimizer to reduce the dose to the critical structures without overweighting the objective and reducing target conformality.

Plan optimization times varied substantially. The main parameters influencing optimization times include the arc length, the size of the target, the size of the dose grid, and whether an intermediate convolution dose is performed for accuracy purposes. The longest optimization time was seen with a lung case with a relatively large target and dose grid. An intermediate convolution dose calculation during optimization was required because of the low density lung. For such cases, multi-threaded or distributed processing for the convolution dose calculation will reduce the overall optimization time to a more clinically viable time as well. Initial tests of compiling the software as a 64-bit program, threading dose calculation, and using two processor cores show performance improvements of roughly 20-30% for dynamic arc plans and 10-20% for IMRT plans.

For a first evaluation of this method of dynamic arc planning, the study was limited to a subset of varying available parameters. The dynamic arcs were planned with a single 360° or less rotation, and used continuously varying MLC segments, varying dose rate, and constant gantry speed. Sensitivity to parameters such as collimator angle, couch angle, arc length, and delivery time were not explored methodically and may provide plan quality improvements in some cases. In addition, there may be a need for multiple arcs in several cases not included in this study: 1) large targets that exceed the MLC aperture size, 2) cases with more than three target levels, 3) multiple targets that do not all fit within the MLC aperture, 4) non-coplanar arcs, and 5) constant dose rate, constant gantry speed arcs. Determining optimal use of these parameters, and potential automation of parameter settings, is subject to ongoing investigation.

Conclusion

An efficient method for dynamic arc or VMAT planning was developed that is generic to different vendor linear accelerators provided they have the ability to move MLC leaves, vary dose rate, and gantry speed simultaneously during dose delivery. In this study, single dynamic arcs were planned with a 360° or less sequence and had continuously varying MLC segments, varying dose rate, and a constant gantry speed. Results from 10 treatment studies demonstrated plan quality similar to, or better than, traditional step-and-shoot IMRT, with estimated delivery times between 70 and 160 seconds for prostate, head and neck, brain, lung, and tonsil studies. Plan monitor units were reduced by up to 23% with the exception of one prostate case for dynamic arc plans. Typical planning optimization times ranged from 5 to 35 minutes.

Acknowledgments

The authors would like to thank the clinical research collaborators for useful feedback and discussions on the prototype software, Erik Sterner and Camilla Blumenthal, RaySearch Laboratories, for development support, and Jim Schewe, Lisa Beckett and Kevin Reynolds, Philips Healthcare, for support with plan evaluation and figure generation. Finally we would like to thank the University of Wisconsin, Virginia Commonwealth University, and MD Anderson for providing the clinic cases used in this study.

Optimization of SmartArc control points in various arc delivery modes

1. Introduction

Plans can be created for all Elekta and Varian linacs that are capable of delivering rotational therapy, This includes most models currently in use in clinics:

- Most Elekta machines
- Varian machines upgraded to be RapidArc-capable
- Non-upgraded Varian machines

As input to the optimization the user can specify one or more arcs with any setting of gantry, couch, collimator, start and stop angles, and more. The user can also set up one arc and have SmartArc create a dual arc plan where the second arc has the same setup as the first, but rotates in the opposite direction. The algorithm behind the dual arc feature strives to reduce leaf travel by distributing control points between the two arcs based on the shapes of the segments. This generally leads to better target coverage and organs at risk sparing for complex cases.

2. Optimization variables, bounds and linear constrations

This section provides additional detail on the optimization of SmartArc control points in different delivery modes and for different linear accelerators.

2.1. Variable definitions

i = Control point index

n = Number of control points in arc

k = Leaf index

lb = Lower bound

ub = Upper bound

$l_{i,k}$ = Leaf position for control point index i and leaf index k

$\overline{l}$ = Vector of all leaf position in all control points

$v_{i,k}$ = Leaf speed for control point index i and leaf index k

v_{max} = Maximum allowed leaf speed

t_i = Control point delivery time

t_{arc} = Total arc delivery time

d_i = Control point dose rate

MU_i = Control point MU

$\overline{MU}$ = Vector of control point MUs

MU_{arc} = Total arc MU

ω_i = Control point gantry speed

ω_{max} = Maximum allowed gantry speed

ω_{min} = Minimum allowed gantry speed

$\Delta\omega_{max}$ = Maximum allowed gantry speed change between control points (deg/s/CP)

$\Delta\theta_i$ = Control point gantry angle interval

$\Delta\theta_{arc}$ = Total arc gantry angle interval from start to stop

η_{min} = Minimum allowed MU per leaf travel $[MU/cm]_{min}$

δ_{max} = Maximum allowed leaf travel per degree $[cm/deg]_{max}$

μ_{max} = Maximum allowed MU per degree $[MU/deg]_{max}$

μ_{min} = Minimum allowed MU per degree $[MU/deg]_{min}$

d_{max} = Maximum allowed dose rate

d_{min} = Minimum allowed dose rate

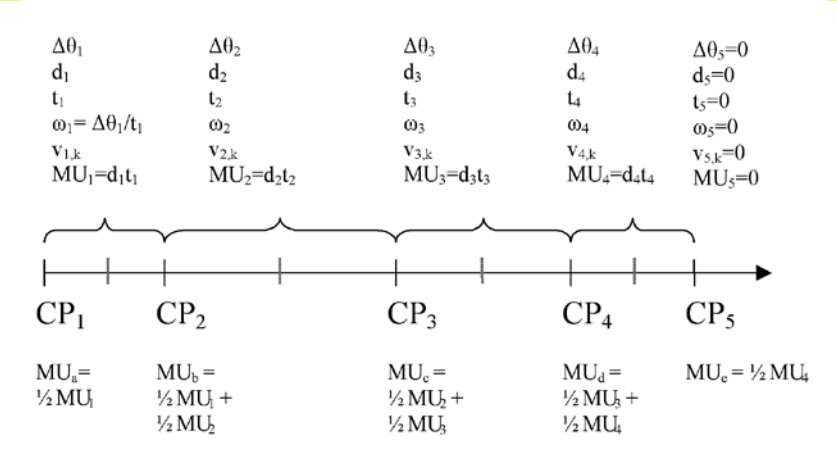

Table 1

In Table 1, CP_1 through CP_5 are the control points. The algorithm assumes that the dose rate (d_i), gantry angle speed (ω_i), and leaf speed ($v_{i,k}$) of each leaf k is constant in the gantry angle interval $\Delta\theta_i$ between control points with index i and i+1.

Control point MUs (MU_1 through MU_5)

Control point monitor units MU_i are defined as the monitor units that are to be delivered between this control point CP_i and the next control point $CP_{(i+1)}$. The last monitor unit, MU_5 in the example, is zero since there is no next control point CP_6. The CP_i are displayed in the UI.

All checks against machine constraints involving *MU* (for example, min and max MU/s, min and max MU/deg, and min MU/cm) are based on the control point MUs.

Dose MUs (MU_a through MU_e)

When dose is computed (both SVD dose during optimization and the accurate dose calculation) MU_a through MU_e are used instead of MU_1 through MU_5. This is a way of compensating for the fact that the leaves move from one control point to the next. For example, passed half way between CP_1 and CP_2 the shape of the segment is more like CP_2 than CP_1, and therefore the MUs need to be shifted to compensate for this.

DICOM cumulative meterset

MUs are exported from Pinnacle in the form of cumulative meterset values that indicate at what MU the machine should be at a certain gantry angle. These are computed by setting the first one to 0 and then adding the control point MU for each control point. See the example in Table 2.

The last CP

CP_5 is the last control point in the arc in this example. It has information about what angle to stop at, what positions the leaf shall be placed at, and a cumulative MU. For this CP dose rate, delivery time and hence control point MU are all 0 since the arc stops here.

CP index	1	2	3	4	5	Total
Gantry angle	0	4	8	12	16	
CP $MU_{(1-5)}$	4	2	6	3	0	15*
Dose $MU_{(a-e)}$	2	3	4	4.5	1.5	15*
DICOM cumulative meterset	0	4	6	12	15	15*

* These three MUs always end up the same.

Table 2

2.2 Elekta

After control points have been created the optimization is divided into two phases with a transition in between.

- Phase 1: Dose rates are allowed to take any value in the range between the highest and the lowest discrete values in the table. Control point MU, arc delivery time, and leaf positions are optimized. Details are given below.
- Transition performed seven iterations from max iterations: The dose rate of each CP is set to the closest discrete value.
- Phase 2: Dose rates for each CP are locked to the discrete value assigned during the transition. The arc delivery time and leaf positions are optimized. Details are in Table 3. At the beginning of this phase the composite objective function value is increased slightly since the dose rates have been modified. This can be seen as a jump in the progress of optimization plot. Most or all of this effect is compensated for during the iterations in this phase.

2.2.1 Elekta Phase 1

The MU of each control point (except the last one which always has zero MU), the arc delivery time, and the leaf positions are free variables. The gantry speed is constant through the arc which means that the control point delivery time is calculated from the gantry angles and the total arc delivery time. The dose rate of each control point may take any value between min and max dose rate, and the dose rate may differ between the control points. The control point dose rate is calculated from the control point MU and the arc delivery time.

Free variables: $\overline{MU}$, t_{arc}, $\overline{I}$

CP delivery time: $t_i = \frac{\Delta\theta_i}{\Delta\theta_{arc}} t_{arc}$

CP MU: MU_i

CP dose rate: $d_i = \frac{MU_i}{\frac{\Delta\theta_i}{\Delta\theta_{arc}} t_{arc}}$

Table 3

Optimization problem definition

Minimize $f(D(MU, l))$

subject to
$MU_{i,lb} \le MU_i \le MU_{i,ub}$ (MU bounds)
$t_{arc,lb} \le t_{arc} \le t_{arc,ub}$ (Delivery time bounds)
$l_{i,k,lb} \le l_{i,k} \le l_{i,k,ub}$ (Leaf position bounds)
$|l_{i,k} - l_{i+1,k}| - v_{max} \frac{\Delta\theta_i}{\Delta\theta_{arc}} t_{arc} \le 0$ (Leaf travel constraint [cm/s])
$|l_{i,k} - l_{i+1,k}| - \frac{1}{\eta_{min}} MU_i \le 0$ (Minimum MU per leaf travel [MU/cm])
$|l_{i,k} - l_{i+1,k}| \le \delta_{max} \Delta\theta_i$ (Maximum leaf travel per gantry degree [cm/deg])
$MU_i - d_{max} \frac{\Delta\theta_i}{\Delta\theta_{arc}} t_{arc} \le 0$ (Maximum dose rate [MU/s])
$d_{min} \frac{\Delta\theta_i}{\Delta\theta_{arc}} t_{arc} - MU_i \le 0$ (Minimum dose rate [MU/s])

(Regular DMPO constraints like minimum gap and interdigitation are left out here)

, where
$MU_{i,ub} = \mu_{max} \Delta\theta_i$
$MU_{i,lb} = \max(MU_{CP,min}, \mu_{min} \Delta\theta_i)$
$t_{arc,ub} = \min(t_{max}, \frac{\Delta\theta_{arc}}{\omega_{min}})$
$t_{arc,lb} = \frac{\Delta\theta_{arc}}{\omega_{max}}$

2.2.2 Elekta Phase 2

The arc delivery time and leaf positions are free variables. The dose rate of each control point is locked to a discrete value which may differ between the control points. The gantry speed is constant through the arc and is calculated from the arc delivery time and the gantry angles. The MU of each control point is no longer a variable as in phase 1 but is instead calculated from its dose rate and delivery time. The previous bounds and linear constraints on MU are now translated into bounds and linear constraints on arc delivery time.

Free variables: $t_{arc}, \overline{l}$

CP delivery time: $t_i = \frac{\Delta\theta_i}{\Delta\theta_{arc}} t_{arc}$

CP MU: $MU_i = \hat{d}_i \frac{\Delta\theta_i}{\Delta\theta_{arc}} t_{arc}$

CP dose rate (discrete): $d_i = \hat{d}_i \in \{ d_1, d_2, ..., d_N \}$

Optimization problem definition

Minimize $f(\overline{D}(t_{arc}, \overline{l}))$

subject to
$t_{arc,lb} \le t_{arc} \le t_{arc,ub}$ (Leaf travel bounds)
$l_{i,k,lb} \le l_{i,k} \le l_{i,k,ub}$ (Delivery time bounds)
$|l_{i,k} - l_{i+1,k}| - \min(v_{max} \frac{\Delta\theta_i}{\Delta\theta_{arc}}, \frac{1}{\eta_{min}} \hat{d}_i \frac{\Delta\theta_i}{\Delta\theta_{arc}}) t_{arc} \le 0$
$|l_{i,k} - l_{i+1,k}| \le \delta_{max} \Delta\theta_i$ (Maximum leaf travel per gantry degree [cm/deg])

, where
$MU_{i,ub} = \mu_{max} \Delta\theta_i$
$MU_{i,lb} = \max(MU_{CP,min}, \mu_{min} \Delta\theta_i)$
$t_{arc,ub} = \min(\frac{\Delta\theta_{arc}}{\omega_{max}}, \frac{MU_{i,lb}}{\hat{d}_i})$
$t_{arc,lb} = \max(\frac{\Delta\theta_{arc}}{\omega_{max}}, \frac{MU_{i,lb}}{\hat{d}_i})$

2.3 Varian—constant dose rate

After control points have been created the optimization is divided into two phases with a transition in between:

- Phase 1: Similar to Elekta phase 1 but dose rates for all CPs are kept identical to each other (any value in the valid range). Total arc MU is optimized instead of CP MU, together with arc delivery time and leaf positions.
- Transition performed seven iterations from max iterations: The dose rate of each CP is set to the closest discrete table value that is lower than the current value and the delivery time is increased with the same factor to yield the same MU. For example, if all dose rates are at 313 MU/min they are shifted to the discrete value 300 MU/min and the delivery time is increased by a factor of 313/300, therefore the user specified maximum delivery time is not taken into account in the next phase. If the dose rates are very close to a higher discrete value, that value is used and then the delivery time is reduced somewhat. Reducing the delivery time may result in leaf positions becoming infeasible due to machine constraints such as maximum leaf speed (cm/s).This is then taken into account.
- Phase 2: Same as Elekta phase 2.

2.4 Varian—variable dose rate, constant gantry speed

After control points have been created the optimization is divided into two phases, both very similar to Elekta phase 1. Nothing is done to the dose rates in the transition, they maintain their variable values within the valid range, and are optimized further in phase 2.

2.5 Varian—variable dose rate, variable gantry speed

In this mode three phases are used. The first transition takes place five iterations after the conversion iteration, and the second seven iterations before max iterations.

In all phases control point MUs and leaf positions are optimized. At each transition, and at the start of phase 1, it is determined which control points are to be locked to the maximum dose rate and which are to be locked to the maximum gantry speed.

The control point dose rate and the control point delivery time are calculated differently depending on whether the dose rate or gantry speed is locked to its maximum value. This also affects the formulation of some of the variable bounds and linear constraints.

For the control points locked to maximum dose rate the gantry speed is allowed to be reduced from the maximum gantry speed so that the control point MU can be increased. The gantry speed variation between control points is limited, which means that there is an additional linear constraint that can be derived from:

$$|\omega_{i+1} - \omega_i| \leq \Delta\, \omega_{max}$$

This constraint couples MU of adjacent control points for which the gantry speed is allowed to vary. The following bound is applied to make sure that the maximum gantry speed is not violated:

$$MU_i \geq d_{max} \frac{\Delta\theta_i}{\omega_{max}}$$

For the control points locked to maximum gantry speed the dose rate is allowed to be reduced from the maximum dose rate so that the control point MU can be decreased. The following bound is applied to make sure that the maximum dose rate is not violated:

$$MU_i \leq d_{max} \frac{\Delta\theta_i}{\omega_{max}}$$

3. Multiple arcs

SmartArc is designed to optimize multiple arcs simultaneously. Multiple arcs can be optimized in two different ways—either the properties of all arcs are defined individually by the user, or dual arcs are generated by a conversion algorithm.

3.1 User specified multiple arcs

The user may set up any number of arcs to optimize. The arcs may cover different gantry angle intervals and rotate in the clockwise or counterclockwise direction.

All arcs are treated as individual arcs and optimized simultaneously. If two arcs cover the same gantry angles, it is likely that the fluence profiles of the two arcs at conversion are very similar resulting in similar segments around the arc, which is not an optimal starting point for the optimization. Therefore, this feature is primarily useful when multiple arcs with no or limited overlap are desired.

For machines where *Allow jaw motion* can be unchecked, it is possible to create multiple arcs that cover different parts of the target (or different targets) by manually setting the jaws prior to starting the optimization. It can be difficult to find the appropriate jaw positions though depending on the location of the isocenter.

3.2 Dual arc

A SmartArc plan can also be set to create two coplanar arcs that focus on different target regions. The first arc rotates in the selected direction and the second in the opposite direction. In this manner the machine gantry does not need to be reset before delivery of the second arc.

Only one set of fluence profiles are optimized for an arc selected to be optimized as a dual arc just as for the single arc case. At conversion time about five control points are created for each initial angle compared to the 2-4 for a single arc, keeping more information from the fluence maps. One or two control points from each initial angle are assigned to each arc according to an algorithm that both considers the center of gravity along the x-axis of each control point and the leaf travel. This, to a large extent, generates one arc where the leaves are distributed to the left and a second where they are distributed to the right in the MLC, in a way that minimizes the leaf travel.

There are advantages to this strategy when an organ at risk (OAR) such as spinal cord or rectum divides the target in a left and a right side. If a single arc is used, control points both to the left and to the right of the OAR are created to make sure that the target coverage is met. The leaf openings must in this case travel back and forth over the OAR increasing the dose to the OAR. Using dual arcs one arc will focus on the left side of the target and one on the right side, reducing the leaf openings over the OAR and thereby the dose delivered to it. User specified multiple arcs will normally behave as single arcs in this respect, as there is no force that drives the segments to be distributed in a left and right manner at conversion.

References

1 Yu CX. Intensity-modulated arc therapy with dynamic multi-leaf collimation: an alternative to tomotherapy. Phys Med. Biol. 40, 1435-1449 (1995).

2 Otto K. Volumetric modulated arc therapy: IMRT in a single gantry arc. Med. Phys. 35, 310-317 (2008).

3 Shepard DM, Cao D, and Afghan MKN. An arc-sequencing algorithm for intensity modulated arc therapy. Med. Phys. 34, 464-470 (2007).

4 Earl MA, Shepard DM, Naqvi S, Li XA, and Yu CX. Inverse planning for intensity-modulated arc therapy using direct aperture optimization. Phys. Med. Biol. 48, 1075-1089 (2003).

5 Ma L, Yu CX, Earl M, et al. Optimized intensity-modulated arc therapy for prostate cancer treatment. Int J. Cancer 96, 379-384 (2001).

6 Duthoy W, Gersem WD, Vergote K, et al. Whole abdominopelvic radiotherapy (WAPRT) using intensity-modulated arc therapy (IMAT): first clinical experience. Int. J. Radiation Oncology Biol. Phys. 57, 1019-1032 (2003).

7 Duthoy W, Gersem WD, Vergote K, et al. Clinical implementation of intensity-modulated arc therapy (IMAT) for rectal cancer. Int. J. Radiation Oncology Biol. Phys. 60, 794-806 (2004).

8 Wong E, D'Souza DP, Chen J, et al. Intensity-modulated arc therapy for treatment of high-risk endometrial malignancies. Int. J. Radiation Oncology Biol. Phys. 61, 830-841 (2005).

9 McNutt T. Dose calculations: collapsed cone convolution superposition and delta pixel beam. Philips White Paper No. 4535 983 02474 (2002).

10 Luan S, Wang C, Chen DZ, Hu XS, Naqvi SA, Yu CX, and Lee CL. A new MLC segmentation algorithm/software for step-and-shoot IMRT delivery. Med. Phys. 31, 695-707 (2004).

11 Gill PE, Murray W, Saunders MA, Wright MH. User's guide for NPSOL 5.0: a Fortran package for nonlinear programming. Report SOL 86-1 (1986).

12 Hårdemark B, Liander A, Rehbinder H, Loef J, Robinson D. P^{3}IMRT. Direct machine parameter optimization. Philips White Paper No. 4535 983 02483 (2004).

13 Bortfeld T, Schlegel W, and Rhein B. Decomposition of pencil beam kernels for fast dose calculations in three-dimensional treatment planning. Med. Phys. 20, 311–318 (1993).

14 Lee N, et al. A phase II study of concurrent chemoradiotherapy using three-dimensional conformal radiotherapy (3D-CRT) or intensity-modulated radiation therapy (IMRT) + Bevacizumab (BV) for locally or regionally advanced nasopharyngeal cancer. Radiation Therapy Oncology Group (RTOG) 0615 (2007).

15 Michalski J, et al. A phase III randomized study of high dose 3D-CRT/IMRT versus standard dose 3D-CRT/IMRT in patients treated for localized prostate cancer. Radiation Therapy Oncology Group (RTOG) 0126 (2004).

16 Bradley J, et al. A randomized phase III comparison of standard dose (60 Gy) versus high dose (74 Gy) conformal radiotherapy with concurrent and consolidation carboplatin/paclitaxel in patients with stage IIIA/IIIB non-small cell lung cancer. Radiation Therapy Oncology Group (RTOG) 0617 (2008).

17 Brachman DG, et al. A phase I/II trial of temozolomide, motexafin gadolinium, and 60 Gy fractionated radiation for newly diagnosed supratentorial glioblastoma multiforme. Radiation Therapy Oncology Group (RTOG) 0513 (2008).

18 B Hårdemark, Liander A, Rehbinder H, Loef J, Robinson D. IMRT. Biological optimization and EUD. Philips White Paper No. 4535 983 02482 (2004).

19 Bzdusek K, Kaus M, Schewe J, Beckett L, and Meltsner M. An efficient approach To volumetric modulated arc therapy optimization and sequencing. Med. Phys. 35 (6), 2867-2867 (2008).

20 Bzdusek K, Friberger H, Eriksson K, Hårdemark B, Robinson D, and Kaus M. Development and evaluation of an efficient approach to volumetric arc therapy planning, Med. Phys. 36 (6), p. 2328-2339 (2009).

Please visit www.philips.com/radiationoncology

Philips Healthcare is part of Royal Philips Electronics

www.philips.com/healthcare
healthcare@philips.com
fax: +31 40 27 64 887

Printed in The Netherlands
4522 962 53751 * JUL 2009

Philips Healthcare
Global Information Center
P.O. Box 1286
5602 BG Eindhoven
The Netherlands